EUV Photochemical Production of Unsaturated Hydrocarbons: Implications to EUV Photochemistry in Titan and Jovian Planets†

Hiroshi Imanaka*,‡,§,⊥ and Mark A. Smith‡,§

Department of Chemistry and Biochemistry, University of Arizona, 1306 East University Boulevard, Tucson, Arizona 85721, Lunar and Planetary Laboratory, University of Arizona, 1629 East University Boulevard, Tucson, Arizona 85721, and SETI Institute, 515 North Whisman Road, Mountain View, California 94043

Received: May 5, 2009; Revised Manuscript Received: July 10, 2009

The EUV photochemistry of methane is one of the dominant chemical processes in the upper atmospheres of Titan and Jovian planets. The dilution of CH_4 with N_2 significantly changes the subsequent hydrocarbon chemistry initiated by EUV photoionization. At wavelengths below 80 nm, the presence of the dominant N_2 species in a N_2/CH_4 gas mixture (=95/5) selectively enhances the formation of unsaturated hydrocarbons, such as benzene and toluene, while pure CH_4 gas leads to a wide mixture of saturated/unsaturated hydrocarbon species. This enhanced formation of unsaturated hydrocarbons is most likely initiated by the generation of CH_3^+ via a dissociative charge-transfer reaction between N_2^+ and CH_4. This mechanism was further confirmed with the dilution of CH_4 with Ar, which shows similarly enhanced formation of unsaturated species from an Ar/CH_4 (=95/5) gas mixture. In contrast, the depleted generation of unsaturated species from a H_2/CH_4 gas mixture (=95/5) suggests that the CH_5^+ ion generated via a proton-transfer reaction is not an important precursor in the production of complex unsaturated hydrocarbons. Therefore, it is the dissociative charge-transfer reaction of CH_4 that initiates the formation of unsaturated complex hydrocarbons through production of $C_2H_5^+$ with subsequent dissociative recombination. Implications regarding photochemistry in the upper atmospheres of Titan and the Jovian planets are discussed.

1. Introduction

The photochemistry of methane in the atmospheres of the outer solar system is important toward the understanding of chemical compositions, thermal balances, and dynamics of the planetary atmospheres. Titan, the organic-rich moon of Saturn, possesses a thick atmosphere of nitrogen with a few percent of methane. This contrasts significantly with the H_2-dominant atmospheres of Jovian planets, such as Jupiter and Saturn. The recent Cassini−Huygens mission shows that a very active organic chemistry occurs in the ionosphere of Titan,[1] suggesting the importance of ionizing energy sources for driving complex organic chemistry. Despite the importance of N_2/CH_4 photochemistry with solar radiation in the EUV−VUV wavelengths, the detailed processes of this complex organic chemistry are not well established. Contrary to the N_2-dominant atmosphere of Titan, less abundant complex molecules have been observed in the H_2-dominant atmospheres of Jupiter and Saturn.[2−4] The processes made possible by N_2 or H_2 buffer in CH_4-containing atmospheres may have significantly differing effects on the gross chemical developments.

The photochemistry induced by photoionization of pure CH_4 gas has long been investigated using discrete line sources from a discharge lamp.[5,6] Continuum light from synchrotron radiation at EUV−VUV wavelengths has been applied to study many methane physical chemical processes in detail, such as ionization yield, partial ionization cross section,[7,8] and dissociative branching of ions.[9] Such studies provide a deep and extensive knowledge of fundamental processes regarding the initial interaction of EUV photons and simple CH_4 molecules. However, the gross features regarding the formation of complex organic molecules developed from those initiation mechanisms are seldom studied in detail.

Current photochemical models,[10−13] combining many single-step investigations of the CH_4 photolysis processes and the rates of radical and ion−molecule reactions, reasonably explain the gross features of the organic inventory of small molecules of C_2-C_4 hydrocarbon species observed in planetary atmospheres. However, because of the complexity of reaction pathways and the limited set of available rates, the formation processes of the heavy hydrocarbons ($>C_4$) are rather based on more speculative assumptions. Recently, we have shown that photoionization of N_2 can play a major role in the formation of complex organic molecules, such as benzene and toluene.[14] However, the detailed chemical mechanisms leading to such complex organic molecules remain to be answered.

When a CH_4-containing gas mixture is irradiated with EUV irradiation, the dilution of CH_4 with N_2 or H_2 may cause significant effects on the subsequent chemistry. The subsequent hydrocarbon chemistry may be strongly dominated by ion−molecule reactions of CH_4 molecules and primary ions from diluted molecules. In this study, the gas-phase products of the EUV irradiations of pure CH_4 and the CH_4 mixtures diluted with N_2, Ar, and H_2 are compared. The initial photoionization processes related to our study are summarized in Table 1.

We hope to demonstrate in this paper the value of direct observation of product distributions as a function of initiating conditions not only for validating those numerical models but also for elucidating the dominant reaction pathways leading to

† Part of the special section "Chemistry: Titan Atmosphere".

* To whom correspondence should be addressed. Address: Department of Chemistry and Biochemistry, University of Arizona, PO Box 210041, 1306 E. University Blvd., Tucson, AZ 85721. Phone: 520-621-4200. Fax: 520-621-8407. E-mail: himanaka@email.arizona.edu.

‡ Department of Chemistry and Biochemistry, University of Arizona.

§ Lunar and Planetary Laboratory, University of Arizona.

⊥ SETI Institute.

10.1021/jp9041952 CCC: $40.75
Published on Web 08/12/2009

TABLE 1: Photoionization Processes Related to the Initial Constituents in This Study

gas species	ionization processes	threshold energy[a]	partial cross sections at 60 nm (Mb)[b]
CH_4	$CH_4 + h\nu \rightarrow CH_4^+ + e^-$	98.3 nm (12.61 eV)	15.3
	$CH_4 + h\nu \rightarrow CH_3^+ + H + e^-$	87.0 nm (14.25 eV)	16.2
	$CH_4 + h\nu \rightarrow CH_2^+ + H_2 + e^-$	81.6 nm (15.20 eV)	0.72
N_2	$N_2 + h\nu \rightarrow N_2^+ + e^-$	79.6 nm (15.58 eV)	22.58
	$N_2 + h\nu \rightarrow N^+ + N + e^-$	51.1 nm (24.26 eV)	
Ar	$Ar + h\nu \rightarrow Ar^+ + e^-$	78.7 nm (15.76 eV)	36.9
H_2	$H_2 + h\nu \rightarrow H_2^+ + e^-$	80.4 nm (15.43 eV)	7.04
	$H_2 + h\nu \rightarrow H^+ + H + e^-$	68.6 nm (18.08 eV)	0.145

[a] Data from ref 15. [b] CH_4 data at 59.9 nm from ref 17, N_2 data at 60.0 nm from ref 18, Ar data at 59.95 nm from ref 23, and H_2 data at 60.48 nm from ref 24.

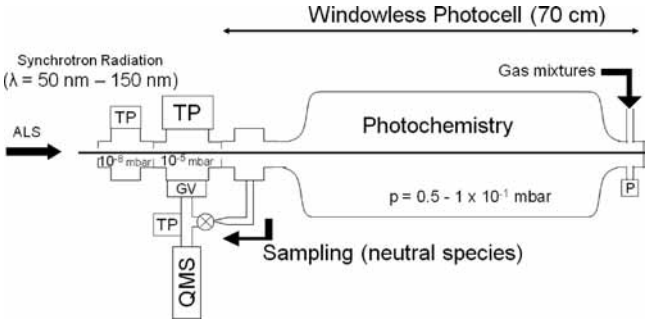

Figure 1. Schematic diagram of the experimental system. Gas mixtures are introduced with a mass flow controller. A windowless photocell is differentially pumped with a series of turbomolecular pumps (TP) through apertures of 1 mm diameter. An EUV−VUV beam of synchrotron radiation (Advanced Light Source) is introduced into the photocell. The irradiation wavelength in this study is controlled from 50 to 100 nm. The neutral gas species produced by photochemistry are analyzed with a quadrupole mass spectrometer (QMS).

complex molecules. Here, the systematic investigations on the final gas-phase photoproducts from various CH_4-containing gas mixtures are presented, and their relations to distinct initiation processes are discussed.

2. Experimental Methods

The experiments are conducted using a tunable narrow band synchrotron radiation source (Chemical Dynamics Endstation, 9.0.2) at the Advanced Light Source (Lawrence Berkeley National Laboratory). The experimental setup is described in our previous paper,[14] and only brief description is given here (Figure 1). A premixed gas mixture is flowed through the windowless photocell chamber of 70 cm length while irradiating the centerline continuously with VUV photons at a selected wavelength. The controlled wavelength of VUV photons in this study is between 50 (24.8 eV) and 100 nm (12.4 eV), and the bandwidth resolution ($E/\Delta E$) is approximately 40. The experimental conditions in this study are listed in Table 2. The neutral gas species produced by photochemistry are sampled through the bypass line near the VUV photon entrance side and are analyzed using a quadrupole mass spectrometer (QMS) (CIS 200, Stanford Research System, CA) with electron impact ionization of 70 eV. Both neutrals and ions are generated in our photocell. Only neutral species are, however, observed with the QMS in this experiment since no nascent ion species are detected without electron impact ionization.

3. Results

3.1. Comparison of Gaseous Products from N_2/CH_4 and CH_4 at 60 nm Irradiation. Mass spectra obtained with 60 nm (20.6 eV) irradiation of the N_2/CH_4 gas mixture and the pure CH_4 gas are shown in Figure 2. The generation of heavy species up to C_8 upon 60 nm irradiation is clearly indicated from comparisons with background mass spectra obtained without EUV irradiation (Figure 2). Despite the 0.05 CH_4 mixing ratio in the N_2/CH_4 gas mixture, generation of such heavy hydrocarbons is as efficient as that in the pure CH_4 irradiation. The remarkable feature observed in the mass spectrum of N_2/CH_4 is the prominent peak of the unsaturated aromatic series, such as benzene and toluene. Contrary to the N_2/CH_4 irradiation, the broad product distribution obtained from CH_4 is interpreted as a mixture of various hydrocarbons of both saturated and unsaturated families. In order to help demonstrate the effect of N_2 dilution in the product distributions, the mass spectral windows in the C_4-C_7 mass range are compared on a linear scale (Figure 3). The QMS intensities are normalized to the relevant initial CH_4 intensities ($m/z = 16$) to demonstrate the conversion efficiency from CH_4 to heavy hydrocarbons. The mass spectral peak distributions in the C_4-C_7 mass ranges show distinct product distributions in H/C ratios. The relative intensities of selected peaks are also shown in Table 2. Formation of unsaturated aromatic hydrocarbons in the N_2/CH_4 gas mixture is 10 times that in the pure CH_4 gas. Thus, it is likely that the presence of N_2 molecules in the initial gas mixture selectively enhances the production of those aromatics. We attribute the above differences in the product distribution to distinct initiation mechanisms. For pure CH_4 gas, the major initiation mechanism with 60 nm irradiation listed in Table 1 leads to nearly equal CH_4^+ and CH_3^+ production.[16,17] For the N_2/CH_4 (=95/5) gas mixture, photoionization of N_2 molecules is dominant since the ratio of ionization cross sections $\sigma(N_2)/\sigma(CH_4)$ at 60 nm is 0.7.[18,19] The primary N_2^+ ion reacts with CH_4 via the dissociative charge transfer reaction

$$N_2^+ + CH_4 \rightarrow N_2 + CH_3^+ + H \qquad (1)$$

Therefore, the dilution with N_2 results in the enhancement of the CH_3^+ ion. Thus, the observed enhancement of unsaturated hydrocarbons from the N_2/CH_4 gas mixture is most likely caused by the enhanced formation of CH_3^+ through the dissociative charge-transfer reaction of CH_4 with N_2^+.

3.2. EUV−VUV Wavelength Irradiation Dependence of Complex Hydrocarbon Formation from N_2/CH_4 and Pure CH_4 Initial Gases. The photoionization thresholds of primary ion formation have been well studied (Table 1). Here, the correlation between the production of complex unsaturated hydrocarbons and the formation of CH_3^+ is investigated with appearance mass spectroscopy. Selected ion species are monitored while the wavelength of VUV irradiation is scanned continuously from 100 to 50 nm (Figure 4).

The remarkable steep rise of H_2, C_2H_2, and C_6H_6 at wavelengths shorter than 80 nm is observed for the N_2/CH_4 gas mixture, which suggests the critical role of N_2 photoionization in the complex organic molecules, as we have shown in our previous publication.[14] On the other hand, H_2 production starts gradually near 85 nm for pure CH_4, which seems to correlate with the formation of CH_3^+ via dissociative photoionization of CH_4.[7,17]

3.3. Gaseous Products from Ar/CH_4 and H_2/CH_4 at 60 nm Irradiation. In order to confirm the role of CH_3^+ in the formation of unsaturated hydrocarbons, we further compare the

TABLE 2: Relative Intensities from Observed Mass Spectra

photocell conditions			without UV irradiation (signal intensity)		60 nm irradiation (relative intensity to initial CH_4)						
gas mixture	mixing ratio (%)	pressure (mbar)	CH_4[a]	dilutant[b]	2	16	26	30	50	56	78
CH_4	100	8.3×10^{-2}	3.04×10^{-04}	none	4.6×10^{-02}	7.7×10^{-01}	1.2×10^{-02}	7.3×10^{-03}	1.5×10^{-04}	9.1×10^{-04}	4.3×10^{-05}
N_2/CH_4	95/5	1.1×10^{-1}	1.81×10^{-05}	3.74×10^{-04}	2.6×10^{-01}	6.0×10^{-01}	8.1×10^{-02}	1.1×10^{-02}	1.0×10^{-03}	1.5×10^{-03}	4.5×10^{-04}
Ar/CH_4	95/5	5.3×10^{-2}	9.35×10^{-06}	2.09×10^{-04}	5.2×10^{-01}	2.2×10^{-01}	5.2×10^{-02}	4.4×10^{-03}	5.0×10^{-04}	3.0×10^{-04}	1.2×10^{-04}
H_2/CH_4	95/5	8.4×10^{-2}	3.44×10^{-05}	7.55×10^{-04}	2.2×10^{01}	7.6×10^{-01}	3.1×10^{-03}	6.3×10^{-03}	1.2×10^{-05}	9.8×10^{-05}	8.2×10^{-06}

[a] CH_4 initial intensities are measured at $m/z = 16$ while UV irradiation is blocked. [b] Initial QMS signal intensities of the dilutant are measured at $m/z = 28$, 40, and 2 for N_2/CH_4, Ar/CH_4, and H_2/CH_4 gas mixtures, respectively.

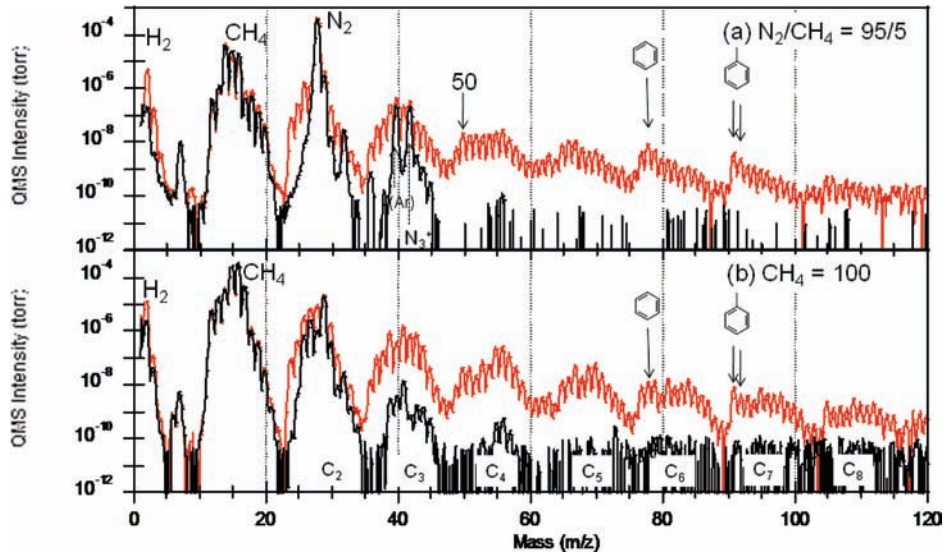

Figure 2. Mass spectra (red lines) of gaseous products obtained with 60 nm irradiation of (a) a $N_2/CH_4 = 95/5$ gas mixture at a pressure of 0.11 mbar and (b) pure CH_4 gas at a pressure of 0.083 mbar. The same gas mixtures without EUV irradiation are also shown as backgrounds (black lines).

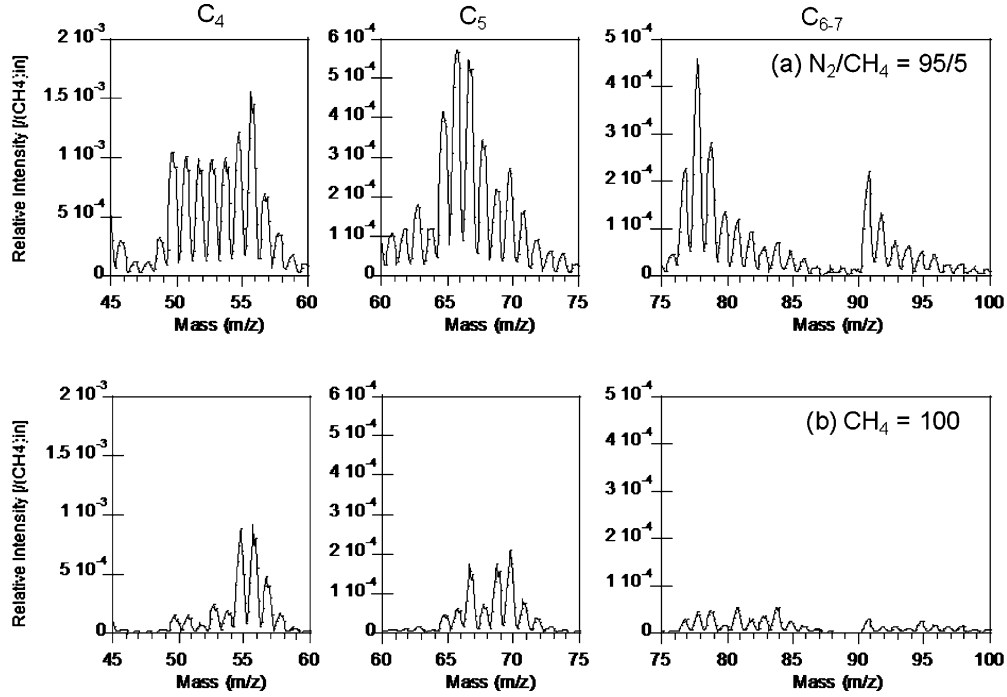

Figure 3. Mass spectral sections of C_4−C_7 clusters obtained with 60 nm irradiation of (a) a $N_2/CH_4 = 95/5$ gas mixture and (b) pure CH_4 gas. The QMS signal intensity upon EUV irradiation is normalized with the initial CH_4 intensity at $m/z = 16$ obtained without EUV irradiation. Imposed figures on the upper right are shown on a linear scale.

products obtained from Ar/CH_4 and H_2/CH_4 gas mixtures with 60 nm irradiation (Figure 5). In the mass spectrum of the irradiated Ar/CH_4 mixture, the mass peaks of Ar^+ (40 and 36) are observed as well as those of Ar^{2+} (20) and Ar_2^+ (80), as expected from our

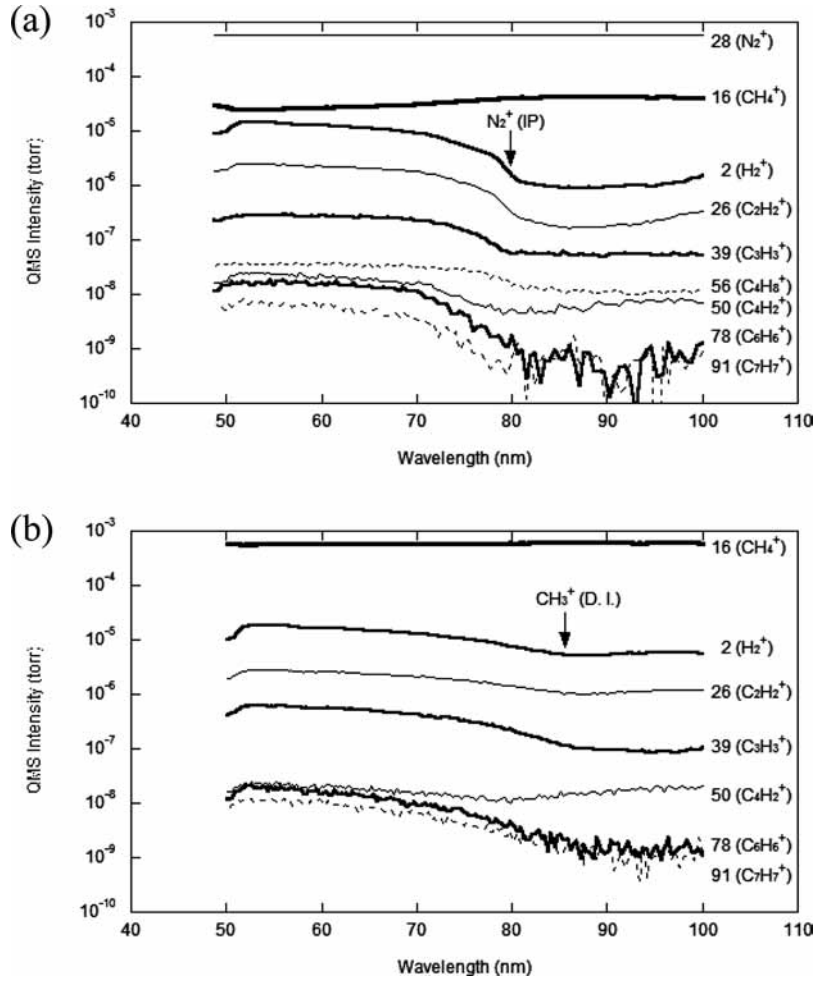

Figure 4. Peak intensities of the selected mass peaks as a function of irradiation wavelength obtained from (a) a $N_2/CH_4 = 95/5$ gas mixture and (b) pure CH_4 gas at a pressure of 0.066 mbar. Tentative assignments of the fragmented ion species are given in parentheses.

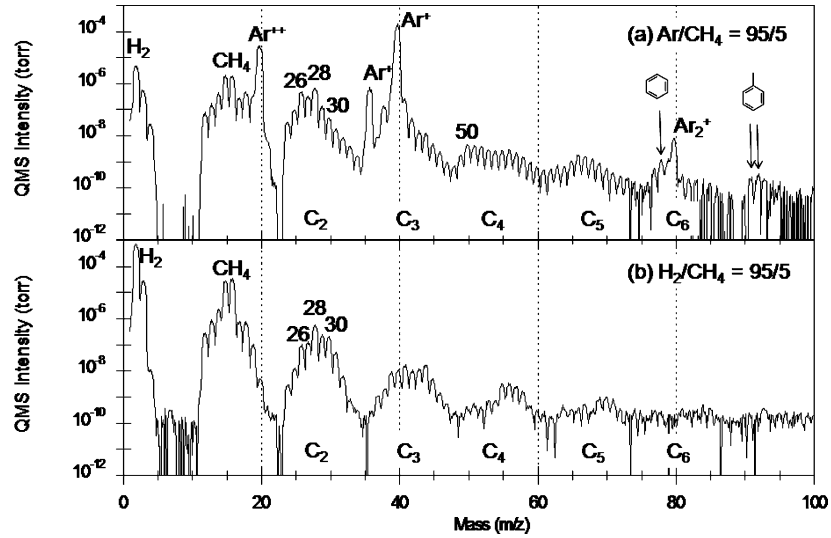

Figure 5. Mass spectra of gaseous products obtained with 60 nm irradiation of (a) a $Ar/CH_4 = 95/5$ gas mixture at a pressure of 0.053 mbar and (b) a H_2/CH_4 =95/5 gas mixture at a pressure of 0.084 mbar.

electron impact ionization (70 eV) mass spectrometry. However, significant production of benzene and toluene at the similar amounts in N_2/CH_4 irradiation (Table 2) is also observed in Ar/CH_4, which is not detected in the H_2/CH_4 gas mixture. Furthermore, the amount of heavy species produced in the H_2/CH_4 gas mixture is much reduced relative to that in Ar/CH_4 mixture irradiation, despite an identical partial pressure of CH_4 molecules. This difference in the yield of complex hydrocarbons from these two gas mixtures implies efficient conversion mechanisms of CH_4 to heavy species only in the Ar/CH_4 gas mixtures and the role of hydrogen in the termination of key channels leading to complex carbonaceous molecules.

The $C_2H_2^+$ (26)/$C_2H_6^+$ (30) peak intensity ratio is 10 in Ar/CH_4, while in H_2/CH_4, it is 0.5 (Table 2). The mass spectral peak distribution of the C_4 ($m/z = 50-58$) region clearly shows

the enrichments of unsaturated C_4H_2 (50) to more saturated hydrocarbons of C_4H_8 (56) and C_4H_{10} (58) in the Ar/CH_4 irradiation compared to those in the H_2/CH_4 irradiation. This variation in C_4 hydrocarbon products indicates that the dilution of CH_4 with Ar enhances the formation of unsaturated hydrocarbons and that most products from H_2/CH_4 tend to be saturated.

Photoionization of Ar leads to the formation of CH_3^+ ion in a similar way to the dissociative charge-transfer reaction of N_2^+ with CH_4 in the N_2/CH_4 gas mixture

$$Ar^+ + CH_4 \rightarrow CH_3^+ + H + Ar \quad (2)$$

The above observations confirm the importance of CH_3^+ in the formation of complex unsaturated molecules. On the other hand, the primary ion of H_2^+ in hydrogen-dominant H_2/CH_4 gas mixtures eventually results in CH_5^+ ion formation

$$H_2^+ + H_2 \rightarrow H_3^+ + H \quad (3)$$

$$H_3^+ + CH_4 \rightarrow CH_5^+ + H_2 \quad (4)$$

Thus, the dilution of CH_4 with H_2 results in the enhancement of CH_5^+ ion formation, which is completely different from the dilutions with N_2 and Ar molecules. This CH_5^+ ion is likely the precursor of saturated hydrocarbons, as observed in Figure 5.

4. Discussion

We have shown that the product distributions of N_2/CH_4 and CH_4 EUV photochemistry at 60 nm are very different in the generation of unsaturated hydrocarbons, and the efficient formation of complex unsaturated species is well correlated to CH_3^+ ion formation. EUV irradiation of the H_2/CH_4 gas mixture at 60 nm implies that the CH_5^+ ion preferentially leads to saturated hydrocarbons with less efficient formation of heavy species. These experiments suggest two distinct chemical pathways induced by CH_3^+ ions and CH_5^+ ions, which may result in the formation of complex unsaturated species and more saturated species, respectively.

In our photocell, the generation of neutral complex organic molecules is a result of a coupled set of photodissociation, photoionization, ion−molecule reaction, electron−ion recombination, and neutral−molecule reaction processes. The precursor ions are first generated in a focal volume with a cross section diameter of approximately 0.1 mm from EUV photoionization. The observation of fluorescence from excited N_2^+ ($B\ ^2\Sigma_u^+$) to N_2^+ ($X\ ^2\Sigma_g^+$) suggests an immediate collisionless expansion of the nascent ion plasma caused by the buildup of space charge to approximately 1 mm diameter within its radiation lifetime of 61 ns.[20] Then, those ions undergo a series of ion−molecule reactions in parallel with electron−ion recombination to generate neutral fragments. The ion densities, n_i, are described as follows

$$\frac{\partial n_i}{\partial t} = \sum_k I\sigma_{i,k}n_k + P_i - L_i n_i - \alpha_i n_i n_e - \frac{D}{\Lambda^2}n_i \quad (5)$$

Here, $\sigma_{i,k}$ is the partial ionization cross section of the ith ionic species from the kth neutral species, and I represents the photon flux. The photon flux, I, is assumed to be 10^{18} photons cm^{-2} s^{-1} based on the typical value of 10^{16} photons sec^{-1} [21] and the area of 1 mm diameter after the initial immediate expansion. Production and loss of ion species by ion−molecule reactions are described as P_i and $L_i n_i$, with α_i being the electron−ion recombination coefficient. D and Λ are the ambipolar diffusion coefficient and characteristic length scale of our photocell chamber, respectively. Table 3 lists the partial ionization cross sections and the relevant reaction rates responsible for determining the major ion densities. Integration of the coupled rate equations suggests that the steady state of the ion species is established to be on the order of 10 μs in our experimental conditions. On this time scale, electron density remains balanced within the total amount of positive ion cloud, and the reduction of electron density by diffusion to the wall is negligible in the pressure range of our experiments. Therefore, the steady-state density of the major ion species can be simply expressed as a function of electron density

$$n_i = \frac{\sum_k I\sigma_{i,k}n_k + P_i}{L_i + \alpha_i n_e} \quad (6)$$

Considering the charge balance equation ($n_e = \sum n_i$), the self-consistent solutions can be iteratively solved. Photoelectrons are assumed to be completely thermalized. This approximation allows for the estimation of the minimum extent for the ion−molecule reaction pathways. The ion−molecule reaction pathways beyond CH_5^+ and $C_2H_5^+$ require the buildup of neutral species (>C_2), which are neglected in the initiation processes in this simple analysis.

Figure 6 shows the calculated number density of the electrons and ionic species as a function of irradiation wavelength for the N_2/CH_4 gas mixture and pure CH_4 gas. In the irradiation of pure CH_4 gas at wavelengths less than 80 nm, both CH_5^+ and $C_2H_5^+$ ions become the most dominant ions, with minor CH_4^+ and CH_3^+ abundances. However, 95% dilution by N_2 molecules has a great effect on the above ion densities at wavelengths shorter than 78 nm. The density of the CH_5^+ ion becomes 20 times smaller than that in the pure CH_4 gas irradiation because of the enlarged CH_4^+−electron recombination. The remarkable increase of CH_3^+ at wavelengths shorter than 78 nm is caused by the dissociative charge-transfer reaction of N_2^+ with CH_4. This 10 times increase in CH_3^+ at around 80 nm correlates well with the 10 times increase in production of neutral species H_2, C_2H_2, and benzene (Figure 4a). This mode change from CH_5^+ to CH_3^+ at around 80 nm supports our previous interpretation of the difference in the product distribution at 60 and 85 nm irradiation.[14] Although the CH_4 partial pressure is only 5% of that in the N_2/CH_4 gas mixture, the ion density of $C_2H_5^+$ is of similar order as that in CH_4 gas irradiation. Through rapid electron−ion recombination rates at these plasma densities, there are direct couplings of each ion with specific neutral end products. Thus, ions of both CH_3^+ and $C_2H_5^+$ are seen to be the key precursor ions in the production of those complex unsaturated hydrocarbons.

The above conclusion is also supported by comparing the initiation processes in various gas mixtures at 60 nm irradiation. The dominant initiation processes at 60 nm irradiation of all of the gas mixtures in this study are summarized in Figure 7. The relative ratios of major ion species estimated from the above referenced calculations are also shown in Figure 7. The estimated ion abundance in the H_2/CH_4 irradiation indicates that the dominant hydrocarbon ion is CH_5^+. The primary ion, H_2^+,

TABLE 3: List of Reactions of Major Ionic Species

										k, α[a]	b.r.	ref
					Photoionization							
p1	N_2	+	$h\nu$	→	N_2^+	+	e^-			($\lambda < 79.6$ nm)		*b*
p2				→	N^+	+	N	+	e^-	($\lambda < 51.1$ nm)		*b*
p3	CH_4	+	$h\nu$	→	CH_4^+	+	e^-			($\lambda < 98.3$ nm)		*c*
p4				→	CH_3^+	+	H	+	e^-	($\lambda < 87.0$ nm)		*c*
p5				→	CH_2^+	+	H_2	+	e^-	($\lambda < 81.6$ nm)		*c*
p6	Ar	+	$h\nu$	→	Ar^+	+	e^-			($\lambda < 78.7$ nm)		*d*
p7	H_2	+	$h\nu$	→	H_2^+	+	e^-			($\lambda < 80.4$ nm)		*e*
p8				→	H^+	+	H	+	e^-	($\lambda < 68.6$ nm)		*e*
					Charge Exchange[f]							
e1	N_2^+	+	CH_4	→	CH_3^+	+	H	+	N_2	1.0×10^{-9}	0.88	*g*
				→	CH_2^+	+	H_2	+	N_2		0.12	
e2	CH_4^+	+	CH_4	→	CH_5^+	+	CH_3			1.1×10^{-9}		*f*
e3	CH_3^+	+	CH_4	→	$C_2H_5^+$	+	H_2			1.1×10^{-9}		*h*
e4	CH_2^+	+	CH_4	→	$C_2H_4^+$	+	H_2			1.3×10^{-9}	0.7	*f*
				→	$C_2H_5^+$	+	H				0.3	
e5	$C_2H_5^+$	+	CH_4	→	$C_3H_7^+$	+	H_2			9.0×10^{-14}		*f*
e6	Ar^+	+	CH_4	→	CH_3^+	+	H	+	Ar	1.0×10^{-9}	0.85	*i*
				→	CH_2^+	+	H_2	+	Ar		0.15	
e7	H_2^+	+	H_2	→	H_3^+	+	H			2.0×10^{-9}		*f*
e8	H_2^+	+	CH_4	→	CH_5^+	+	H			3.8×10^{-9}	0.03	*j*
				→	CH_4^+	+	H_2				0.37	
				→	CH_3^+	+	H_2	+	H		0.6	
e9	H_3^+	+	CH_4	→	CH_5^+	+	H_2			2.4×10^{-9}		*f*
e10	H^+	+	CH_4	→	CH_3^+	+	H_2			4.5×10^{-9}	0.82	*f*
				→	CH_4^+	+	H				0.18	
e11	CH_4^+	+	H_2	→	CH_5^+	+	H			3.5×10^{-11}		*f*
e12	CH_2^+	+	H_2	→	CH_3^+	+	H			1.2×10^{-9}		*f*
					Electron−Ion Recombination[k]							
r1	N_2^+	+	e^-	→	$N(^2D)$	+	$N(^2D, ^4S)$			1.8×10^{-7}		*l*
r2	CH_5^+	+	e^-	→	CH_4	+	H			2.8×10^{-7}	<0.02	*m*
				→	CH_3	+	H_2				0.05	
				→	CH_3	+	2H				0.7	
				→	CH_2	+	H_2	+	H		0.2	
				→	CH	+	$2H_2$				0.05	
r3	CH_4^+	+	e^-	→	CH_3	+	H			3.5×10^{-7}	0.5	*n*
				→	CH_2	+	2H				0.5	
r4	CH_3^+	+	e^-	→	CH_2	+	H			3.5×10^{-7}	0.4	*o*
				→	CH	+	H_2				0.14	
				→	CH	+	2H				0.16	
				→	C	+	H_2	+	H		0.3	
r5	CH_2^+	+	e^-	→	CH	+	H			6.4×10^{-7}	0.25	*p*
				→	C	+	H_2				0.12	
				→	C	+	2H				0.63	
r6	$C_2H_5^+$	+	e^-	→	C_2H_4	+	H			2.8×10^{-7}	0.12	*q*
				→	C_2H_3	+	2H				0.27	
				→	C_2H_2	+	3H				0.13	
				→	C_2H_2	+	H_2	+	H		0.29	
				→	CH_3	+	CH_2				0.17	
r7	H_3^+	+	e^-	→	H_2	+	H			1.2×10^{-7}	0.25	*r*
				→	H	+	H	+	H		0.75	

[a] Reaction rates (cm^3/s) at 300 K. [b] References 18 and 22. [c] Reference 17. [d] Reference 23. [e] Reference 24. [f] Reaction rates and branching ratios are compiled and evaluated in ref 25. [g] Reference 26. [h] Reference 27. [i] Reference 28. [j] Reference 29. [k] Comprehensively reviewed in ref 30. [l] Production of $N(^2D)$ is the main channel.[31] [m] Reference 32. [n] Reference 33. [o] Reaction rate[33] and the branching ratio.[34] [p] Reference 35. [q] The rate and branching ratios are assumed to be same to those of $C_2D_5^+$.[36] [r] Reaction rate[37] and the branching ratios.[38]

immediately reacts with H_2 molecules, generating the H_3^+ ion. The subsequent ion−molecule reaction of H_3^+ with CH_4 is the main pathway to the CH_5^+ ion via a proton-transfer reaction rather than a dissociative charge-transfer reaction. The main neutral fragment through dissociative recombination of the terminal CH_5^+ ion is the CH_3 radical.[32] The observation of low efficiency in heavy hydrocarbon production (Figure 5b) suggests a minor role of CH_3 radicals in the formation of complex molecules. Because the dissociative recombination of the second most abundant H_3^+ ion results in the production of H_2 and H,[38] the atomic H may also inhibit the production of heavy hydrocarbons. In the irradiation of pure CH_4 gas, the dominant ions of CH_5^+ and $C_2H_5^+$ lead to a mixture of heavy saturated/unsaturated hydrocarbons. Comparison with H_2/CH_4 suggests that the buildup of heavy species is likely attributed to $C_2H_5^+$ ions and that CH_3 radical addition to unsaturated molecules may lead to heavy saturated species. In the irradiation of N_2/CH_4 and Ar/CH_4 gas mixtures, almost identical amounts of unsaturated hydrocarbons are preferentially produced (Figures 2a, 5a). This confirms the important role of the dissociative charge-transfer reaction of CH_4 in the formation of unsaturated heavy species. Although the possible ion−molecule chemistry beyond

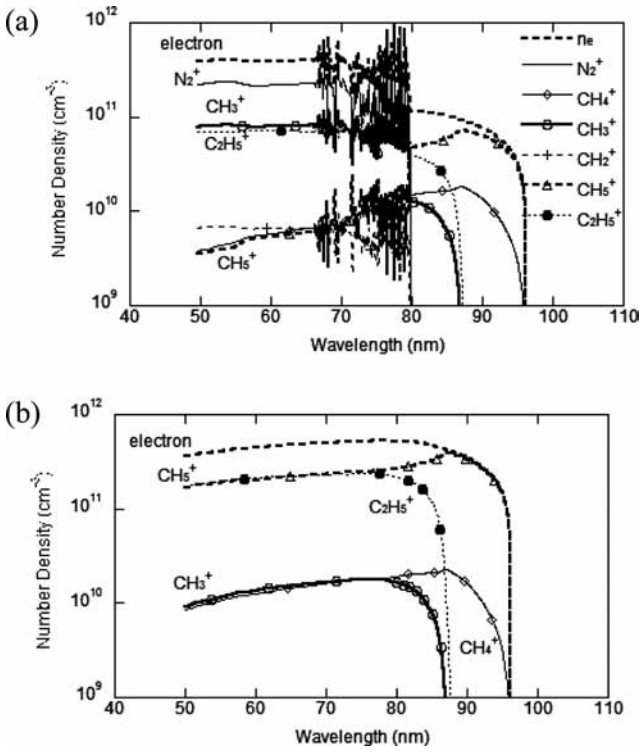

Figure 6. Calculated concentrations of electrons and ionic species in the steady state as a function of irradiation wavelength for (a) a N_2/CH_4 gas mixture and (b) pure CH_4 gas at 0.066 mbar. An average photon flux of $10^{18}h\nu$ cm^{-2} s^{-1} is assumed.

the $C_2H_5^+$ ion is not completely excluded, those CH_3^+ and $C_2H_5^+$ ions predominantly recombine with electrons and generate reactive neutral species with low H/C ratios, such as C_2H_2 and CH,[36] as precursors for heavy hydrocarbons under our experimental conditions. These highly unsaturated species are believed to be precursors for benzene either through neutral reaction or ion−molecule reaction processes. [13,39,40] Thus, the dissociative charge-transfer reaction of CH_4 is the responsible initial step toward the formation of complex unsaturated or aromatic hydrocarbons, such as benzene.

Our conclusion here is limited to the distinct chemical mechanism in the very initial stage, where ion−molecule reactions are one of the dominant factors determining the subsequent chemistry. These ion−molecule reactions have demonstrated weak temperature dependence, and our results from the experiment at 300 K suggest certain implications in the photochemistry of planetary atmospheres in the cold outer solar system environment. Titan, the largest moon of Saturn, possesses a thick atmosphere of nitrogen, containing a few percent of methane. Solar ultraviolet radiation induces a very active organic chemistry in the atmosphere, resulting in a rich suite of heavy hydrocarbons and nitriles. The recent Cassini−Huygens mission detected the remarkable abundance of benzene at mixing ratios near 4 ppm in the ionosphere.[41] Because solar EUV radiation is absorbed by N_2 in the ionosphere, EUV photoionization of N_2 may catalytically generate the complex unsaturated hydrocarbons observed in Titan's upper atmosphere via a dissociative charge-transfer reaction of N_2^+ with CH_4. On the other hand, in the atmospheres of Jupiter and Saturn, hydrogen is dominant, with ratios of $[CH_4]/[H_2]$ in the stratospheres of 1.9×10^{-3} [42] and 5.1×10^{-3},[43] respectively. Those ratios drop down to below 10^{-4} near their homopauses.[44,45] Photochemistry does convert methane to heavy hydrocarbons in these atmospheres[10,13,46] but a much lower percentage of

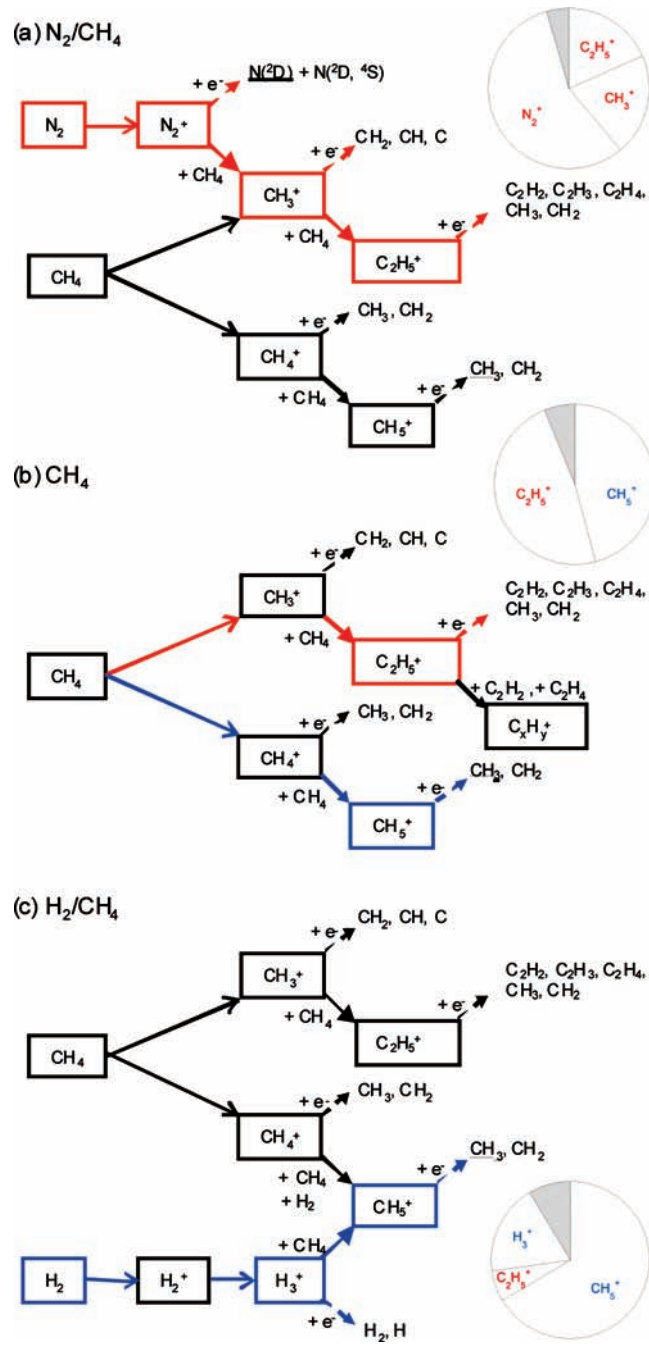

Figure 7. Summary of initial chemical reaction pathways in complex molecule synthesis from EUV irradiation of various methane mixtures. The estimated relative ratios of major ion species and other minor ions (hatched area) are also shown.

C_2-C_4 species are observed than on Titan. Although benzene is detected in the upper atmospheres of Jupiter and Saturn, the abundance is less than 10 ppb at midlatitude.[47] Our experimental results imply that EUV photochemical formation of complex hydrocarbons in the H_2-dominant atmospheres is less efficient and that this diversity of atmospheric organic chemistry seen in the N_2-dominant atmosphere of Titan and the H_2-dominant atmospheres of Jupiter and Saturn could originate from the differences in the photoinduced ion chemistry of CH_4.

5. Conclusion

We have conducted a series of experiments investigating the EUV photochemistry of CH_4 in various gas mixtures. The

product distributions of N_2/CH_4 (=95/5) and pure CH_4 EUV photochemistry at 60 nm change significantly, and the efficient formation of complex unsaturated species is well correlated with CH_3^+ ion formation. Similar enhanced formation of unsaturated species is also observed at 60 nm irradiation of an Ar/CH_4 (=95/5) gas mixture. This enhanced formation of unsaturated hydrocarbons is most likely initiated by the generation of CH_3^+ via a dissociative charge-transfer reaction of CH_4. In contrast, 60 nm irradiation of a H_2/CH_4 gas mixture (=95/5) indicates that the CH_5^+ ion formed via a proton-transfer reaction to CH_4 preferentially leads to saturated hydrocarbons with less efficient formation of heavy species. The diversity of atmospheric organic chemistry seen in the N_2-dominant atmosphere of Titan and the H_2-dominant atmospheres of Jupiter and Saturn could originate from the difference in the pathways induced by dissociative charge-transfer and proton-transfer reactions of CH_4. EUV photoionization of N_2 may catalytically generate the complex unsaturated hydrocarbons observed in Titan's upper atmosphere via the dissociative charge-transfer reaction of CH_4.

Acknowledgment. This work was supported by the NASA Exobiology Program Grant NNG05GO58G, the Directors Research and Development Fund, Jet Propulsion Laboratory, and the National Science Foundation through Grant CHE-0513364. H.I. is also partially supported by the NASA Exobiology Program Grant NNG05GQ68. The Advanced Light Source is supported by the Director, Office of Science, Office of Basic Energy Sciences, of the U.S. Department of Energy under Contract No. DE-AC02-05CH11231. Drs. Mike Jimenez-Cruz, Kevin Wilson, Musa Ahmed, and Mr. Bruce Rude are greatly acknowledged for their assistance and advice at the ALS. We thank Lee Macomber, Ed Autz, Doug Archer, Zachary Scott, and Dr. George Tikhonov for their assistance.

References and Notes

(1) Waite, J. H., Jr.; et al. *Science* **2005**, *308*, 982.
(2) Moses, J. I.; Fouchet, T.; Bezard, B.; Gladstone, G. R.; Lellouch, E.; Feuchtgruber, H. The stratosphere of Jupiter. In *Jupiter: Planet, Satellites and Magnetosphere*; Bagenal, F., McKinnon, W. B., Dowling, T., Eds.; Cambridge Univ. Press: New York, 2004; p 129.
(3) Yelle, R. V.; Miller, S. Jupiter's Thermosphere and Ionosphere. In *Jupiter: Planet, Satellites and Magnetosphere*; Bagenal, F., Dowling, T., McKinnon, W. B., Eds.; Cambridge Univ. Press: New York, 2004; p 185.
(4) Encrenaz, T. *Space Sci. Rev.* **2005**, *116*, 99.
(5) Jensen, C. A.; Libby, W. F. *J. Chem. Phys.* **1968**, *49*, 2831.
(6) Walker, D. C.; Back, R. A. *J. Chem. Phys.* **1963**, *38*, 1526.
(7) Chupka, W. A. *J. Chem. Phys.* **1968**, *48*, 2337.
(8) Chupka, W. A.; Berkowitz, J. *J. Chem. Phys.* **1971**, *54*, 4256.
(9) Stockbauer, R. *J. Chem. Phys.* **1973**, *58*, 3800.
(10) Yung, Y. L.; DeMore, W. B. *Photochemistry of Planetary Atmospheres*; Oxford Univ. Press: New York, 1999.
(11) Atreya, S. K. *Atmospheres and Ionospheres of the Outer Planets and Their Satellites*; Springer-Verlag: New York, 1986.
(12) Wilson, E. H.; Atreya, S. K. *J. Geophys. Res.* **2004**, *109*, E06002.
(13) Moses, J. I.; Fouchet, T.; Bezard, B.; Gladstone, G. R.; Lellouch, E.; Feuchtgruber, H. *J. Geophy. Res.* **2005**, *110*, E08001.
(14) Imanaka, H.; Smith, M. A. *Geophys. Res. Lett.* **2007**, *34*, L02204.
(15) Berkowitz, J. *Photoabsorption, Photoionization, and Photoelectron Spectroscopy*; Academic Press: New York, 1979.
(16) Latimer, C. J.; Mackie, R. A.; Sands, A. M.; Kouchi, N.; Dunn, K. F. *J. Phys. B: At. Mol. Opt. Phys.* **1999**, *32*, 2667.
(17) Samson, J. A. R.; Haddad, G. N.; Masuoka, T.; Pareek, P. N.; Kilcoyne, D. A. L. *J. Chem. Phys.* **1989**, *90*, 6925.
(18) Samson, J. A. R.; Masuoka, T.; Pareek, P. N.; Angel, G. C. *J. Chem. Phys.* **1987**, *86*, 6128.
(19) Kameta, K.; Kouchi, N.; Ukai, M.; Hatano, Y. *J. Electron Spectrosc. Relat. Phenom.* **2002**, *123*, 225.
(20) Huber, G.; Herzberg, G. *Molecular Spectra and Molecular Structure IV, Constants of Diatomic Molecules*; Van Nostrand: New York, 1979.
(21) Heimann, P. A.; et al. *Rev. Sci. Instrum.* **1997**, *68*, 1945.
(22) Fennelly, J. A.; Torr, D. G. *At. Data Nucl. Data Tables* **1992**, *51*, 321.
(23) Samson, J. A. R. The Measurement of the Photoionization Cross Sections of the Atomic Gases. In *Advances in Atomic and Molecular Physics*; Bates, D. R., Estermann, I., Eds.; Academic Press: New York, 1966; Vol. 2, p 177.
(24) Chung, Y. M.; Lee, E. M.; Masuoka, T.; Samson, J. A. R. *J. Chem. Phys.* **1993**, *99*, 885.
(25) Anicich, V. G. *J. Phys. Chem. Ref. Data* **1993**, *22*, 1469.
(26) Anicich, V. G.; Wilson, P.; McEwan, M. J. *J. Am. Soc. Mass Spectrom.* **2004**, *15*, 1148.
(27) Anicich, V. G.; Wilson, P.; McEwan, M. J. *J. Am. Soc. Mass Spectrom.* **2003**, *14*, 900.
(28) Anicich, V. G.; Laudenslager, J. B.; Huntress, J. W. T.; Futrell, J. H. *J. Chem. Phys.* **1977**, *67*, 4340.
(29) Kim, J. K.; Huntress, W. T., Jr. *J. Chem. Phys.* **1975**, *62*, 2820.
(30) Florescu-Mitchell, A. I.; Mitchell, J. B. A. *Phys. Rep.* **2006**, *430*, 277.
(31) Peterson et al. *J. Chem. Phys.* **1998**, *108*, 1978.
(32) Semaniak, J.; et al. *Astrophys. J.* **1998**, *498*, 886.
(33) Mul, P. M.; Mitchell, J. B. A.; D'Angelo, V. S.; Defrance, P.; McGowan, J. W.; Froelich, H. R. *J. Phys. B: At. Mol. Opt. Phys.* **1981**, *14*, 1353.
(34) Vejby-Christensen, L.; Andersen, L. H.; Heber, O.; Kella, D.; Pedersen, H. B.; Shmidt, H. T.; Zajfman, D. *Astrophys. J.* **1997**, *483*, 531.
(35) Larson, Å.; et al. *Astrophys. J.* **1998**, *505*, 459.
(36) Geppert, W.; et al. *Phys. Rev. Lett.* **2004**, *93*, 153201.
(37) Sundstrom, G.; et al. *Science* **1994**, *263*, 785.
(38) Datz, S.; Sundström, G.; Biedermann, C.; Broström, L.; Danared, H.; Mannervik, S.; Mowat, J. R.; Larsson, M. *Phys. Rev. Lett.* **1995**, *74*, 896.
(39) Wilson, E. H.; Atreya, S. K.; Coustenis, A. *J. Geophy. Res.* **2003**, *108*, 5014.
(40) Vuitton, V.; Yelle, R. V.; Cui, J. *J. Geophys. Res. [Planets]* **2008**, *113*.
(41) Waite, J. H., Jr.; Young, D. T.; Cravens, T. E.; Coates, A. J.; Crary, F. J.; Magee, B.; Westlake, J. *Science* **2007**, *316*, 870.
(42) Niemann, H. B.; et al. *Science* **1996**, *272*, 846.
(43) Flasar, F. M.; et al. *Science* **2005**, *307*, 1247.
(44) Yelle, R. V.; Young, L. A.; Vervack, R. J., Jr; Young, R.; Pfister, L.; Sandel, B. R. *J. Geophy. Res.* **1996**, *101*, 2149.
(45) Smith, G. P.; Shemansky, D. E.; Holberg, J. B.; Broadfoot, A. L.; Sandel, B. R. *J. Geophy. Res.* **1983**, *88*, 8667.
(46) Lebonnois, S. *Planet. Space Sci.* **2005**, *53*, 486.
(47) Bezard, B.; Drossart, P.; Encrenaz, T.; Feuchtgruber, H. *Icarus* **2001**, *154*, 492.

JP9041952